CHEMISTRY
A EUROPEAN JOURNAL

DOI: 10.1002/chem.200600920

Structural Characterization of Modern and Fossilized Charcoal Produced in Natural Fires as Determined by Using Electron Energy Loss Spectroscopy

Ilit Cohen-Ofri,*[a] Ronit Popovitz-Biro,[b] and Steve Weiner[a]

Abstract: Charcoal produced in natural fires is widespread, but surprisingly little is known about its structure and stability. TEM and electron energy loss spectroscopy (EELS) were used to characterize the organized graphite-like microcrystallites and amorphous nonorganized phases of modern charcoal that had been produced in natural fires. In addition, a semiordered structure was identified in two modern charcoal samples. Fossilized charcoal contains fewer graphite-like microcrystallites than modern samples. EELS spectra confirmed that the dominant structure in fossilized charcoal is amorphous carbon. EELS measurements also revealed that only the nonorganized phase contains oxygen, which indicates that the degradation of the fossilized charcoal structure occurs mainly through oxidation processes. The few graphite-like microcrystallites found in fossilized charcoal were composed of onion-like structures that are probably less prone to oxidation owing to their rounded structures.

Keywords: charcoal · electron energy loss spectroscopy · electron microscopy · microcrystallites · oxidation

Introduction

Charcoal produced in open fires is of much interest in terms of its role in the carbon cycle of the earth, as an important component of certain soils, and as a source of information on human management of fire in the past.[1–3] Charcoal is also a widely used material for radiocarbon dating of archeological sites.[4,5] Thus, understanding the structure of so-called "natural" charcoal, as well as the manner in which it degrades chemically with time (diagenesis) is important.

Surprisingly little is known about the structure of natural charcoal,[6–8] and almost nothing is known about charcoal diagenesis. In fact, until recently it was not clear whether charcoal did actually degrade with time. Recent field observations and analyses of soil charcoal samples have shown that indeed it does.[5] Our own field observations at archaeological sites, which show an absence of charcoal in some sites where fire was clearly used, or differential preservation in different parts of the site, clearly support the notion that charcoal does indeed degrade over time.

Much more is known about charcoal produced under controlled conditions in ovens and at temperatures well above those that natural fires reach (namely, up to about 900 °C). These studies show that the basic structural motif of charcoal is composed of crystallites of graphite embedded in an amorphous carbon phase.[9–11] The structure of wood charcoal produced at temperatures above 1000 °C was classified as nongraphitizable carbon by Franklin.[12] This classification was attributed to the porous nature of wood, which is believed to cause the random orientation of graphite-like microcrystallites. Ishimaru et al. found that wood charcoal carbonized at 700 °C contains various carbon structures, which include graphite layers, onion-like particles, and diamond structures.[13] Hata et al. showed that onion-like structures form in areas that are dominated by lignin, whereas random structures are found in areas in which the microfibrils (cellulose) of wood are located.[14] However, it was found that the graphite-like microcrystallites show some preferred orientation that might be affected by the cellulose orientation in the native wood cell.[15–17] Porous structures were also observed that show curved, hollow features.[13] The wood charcoal samples observed were produced under highly controlled burning conditions that are very different from those in an open fire,[18] in which the temperatures and oxygen availability can vary significantly.

[a] I. Cohen-Ofri, Prof. S. Weiner
Department of Structural Biology
Weizmann Institute of Science
Rehovot 76100 (Israel)
Fax: (+972) 8-934-4136
E-mail: ilit.cohen-ofri@weizmann.ac.il

[b] Dr. R. Popovitz-Biro
Chemical Research Support Unit
Weizmann Institute of Science
Rehovot 76100 (Israel)

In the past, we have used FTIR and Raman spectroscopies, TEM, thermogravimetric/differential thermal analysis (TGA/DTA), ESR spectroscopy, and resistivity measurements to show that natural wood charcoal (referred to as modern charcoal) is composed of two phases:[7] an organized phase that contains graphite-like microcrystallites (average size 5 nm) and a nonorganized phase (following the terminology used by Franklin[12]) that resembles amorphous carbon. The data obtained by means of these methods were then used to characterize fossilized charcoal samples (mostly associated with hearths) from various archaeological sites.[7] As the modern charcoal samples were produced in simple open campfires and from tree species that were present at these sites in the past,[19] it seems reasonable to directly compare the structures of the modern and the fossilized charcoal specimens. It was found that fossilized charcoal has the same basic structure as the modern samples, but with what appears to be a major reduction in the amount of graphite-like microcrystallites. In contrast to modern charcoal, fossilized charcoal contains additional carboxylic groups; this led us to conclude that the diagenesis of charcoal mainly occurs by means of oxidation, which alters the charcoal structure. The exact nature of the alteration is not known, but it results in the reduction of the relative proportion of graphite-like microcrystallites. The main problem associated with analyzing bulk samples is that the chemical structure of the organized and nonorganized phases is not differentiated.

This study takes advantage of the high-resolving capabilities of TEM and electron energy loss spectroscopy (EELS) to obtain detailed structural and chemical information on the organized and nonorganized phases in modern and fossilized charcoal. The EELS spectra of various polymorphs of crystalline carbon, as well as its amorphous phase, are well documented.[20] In particular, characteristic peaks in the low-loss region of the spectrum, and in the electron-energy-loss near-edge fine structure (ELNES) of the carbon K-edge, were attributed to various bonding and coordination states.[21,22] In addition to the carbon structural properties, the occurrence of other light elements, such as oxygen and nitrogen, was also investigated.

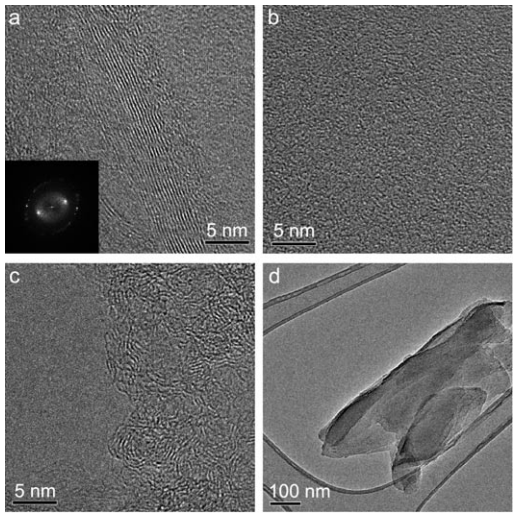

Figure 1. TEM images of modern charcoal samples: a) *Ceratonia* that contains organized and nonorganized phases (inset: fast Fourier transform (FFT) of the organized region); b) nonorganized phase of *Ceratonia* charcoal; c) *Quercus* charcoal showing a semiordered phase; and d) low-magnification image of *Ceratonia* charcoal showing a faceted charcoal flake.

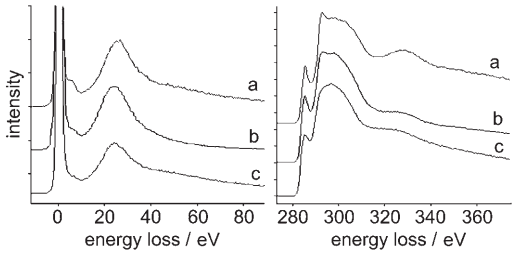

Figure 2. EELS spectra of modern charcoal samples: a) The *Ceratonia* charcoal organized phase reveals the presence of the three characteristic peaks of graphite at 6.5, 284, and 291 eV. b) The *Quercus* charcoal semiordered phase. The peak at 6.5 eV hardly exists, and the peak at 291 eV is present along with the peak at 284 eV. c) The *Ceratonia* charcoal nonorganized phase. An amorphous phase is indicated by the fact that the peak at 6.5 eV hardly exists, the lack of the peak at 291 eV, and the fact that the 284 eV peak is not well separated.

Results and Discussion

Modern charcoal: High-resolution images and EELS spectra were obtained from four modern charcoal samples and five fossilized samples (four from Kebara cave and one from Tel Dor, Israel). The images and spectra obtained for the modern charcoal samples show that variations exist between charcoal samples that are derived from different tree species, and are characterized by two types of structure: a two-phase structure (in *Ceratonia* and *Olea*) and a single-phase semiordered structure (in *Quercus* and *Laurus*). The two-phase structures are composed of an organized phase and a nonorganized phase. The organized phase comprises graphite-like microcrystallite sheets (Figure 1a). Line a in the EELS spectra shown in Figure 2 contains the three main peaks at 6.5, 285, and 291 eV that are characteristic for graphite microcrystallites. The peak observed at 6.5 eV is attributed to the electronic transition from $\pi \rightarrow \pi^*$ levels and can be assigned to C=C bonds (in the low-loss region). That at 285 eV is attributed to the $1s \rightarrow \pi^*$ levels and can be assigned to C=C bonds (the core-loss region), and that at 291 eV is attributed to the transition from $1s \rightarrow \sigma^*$ and can be assigned to the C–C bond.[22] The structure of the nonorganized phase is characterized by a uniform texture (Figure 1b). The EELS spectrum of the nonorganized phase shows the features of amorphous carbon (line c in Figure 2), which is characterized by the existence of some C=C bonds (a weak peak at 6.5 eV in the low-loss region and a less-well-defined peak at 285 eV). The modulations around 290 eV that were attributed to the sigma bond appear to

have merged together in this instance as a result of a disordered environment.[23]

The single-phase semiordered structure is characterized by exfoliated graphene layers and small stacks of 2 to 3 layers, which result in only short-range order (Figure 1c). These features are similar to nongraphitizing (sucrose) single-layer carbon structures reported by Harris et al.[24] The EELS spectrum of the semiordered phase (line b in Figure 2) contains the peak in the low-loss region at 6.5 eV and also the peak at 285 eV in the core region. The peak at 291 eV is very small, but unlike in the amorphous carbon phase, it is distinct, which indicates that the samples contain short-range order and a significant amount of sp^2 hybridization.[25] No significant amount of oxygen was detected in any of the phases of modern charcoal specimens. At low magnification the modern charcoal samples tend to be composed of flat layers (Figure 1d).

The various structures obtained from the modern charcoal samples can be correlated with other properties of modern charcoal that we have observed previously.[7] The *Quercus* and *Laurus* samples contain a homogeneous semiordered structure according to the EELS spectra. These samples were found to contain small amounts of organic residues, as deduced from the relatively high temperature DTA peak values and low resistivity values obtained. We surmise that the structure of the semiordered charcoal (the conjugated double bonds and the relative lack of amorphous material) makes them better conductors. The *Ceratonia* and to some extent *Olea* samples, which according to the EELS spectra have relatively large amounts of amorphous carbon, contain higher amounts of organic residues, based on lower temperature DTA peak values and higher resistivity values.

Fossilized charcoal: Five fossilized charcoal samples (four from Kebara Cave and one from Tel Dor) were examined by means of high-resolution TEM (HRTEM) and EELS. The HRTEM results showed that the amorphous phase (Figure 3a) is much more abundant in the fossilized samples than in the modern samples, which is consistent with the EELS spectra obtained for the fossilized samples (line b in Figure 4). Furthermore, the fossilized amorphous phases all contain oxygen. The ELNES spectrum of the oxygen K-edge comprises two peaks: one at 532 eV that can be attributed to the $1s \rightarrow \pi^*$ transition of a C=O bond and a second peak, at 541 eV, that can be attributed to the $1s \rightarrow \sigma^*$ transition of a C=O bond.[26] Sample CH-16 and an identified fossilized oak (*Quercus*) sample from Kebara Cave (Figure 3a) are composed entirely of amorphous carbon, whereas samples F-19 and CH-4 (Figure 3b) from Kebara Cave, and the sample from Tel Dor (CHI-5) (Figure 3c), also contain small amounts of an organized phase. This organized phase is found mainly in the form of rounded structures that are reminiscent of the porous structures reported from modern-wood charcoal,[13] and observed in our own modern charcoal samples (Figure 5a). We also noted curled structures in the Tel Dor sample that produced EELS spectra that are indicative of ordered and semiordered phases (line a in Figure 4).

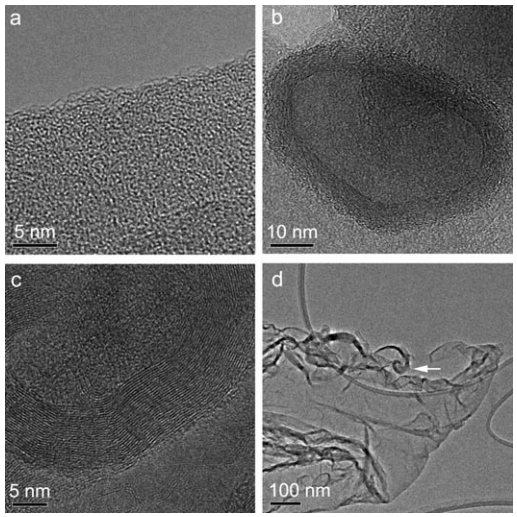

Figure 3. TEM images of fossilized charcoal samples: a) fossilized *Quercus* from Kebara Cave; b) onion-shaped graphite-like microcrystallites from Kebara cave (CH-4); c) curled graphite-like microcrystallites from Dor (CHI-5); d) low-magnification image of Dor charcoal sample (CHI-5).

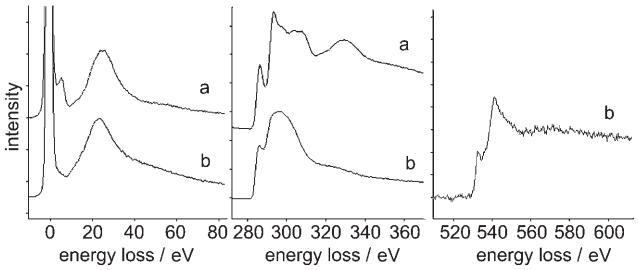

Figure 4. EELS spectra of fossilized charcoal samples: a) The Dor (CHI-5) onion-like organized phase reveals the presence of the three characteristic peaks of graphite at 6.5, 284, and 291 eV. No oxygen was detected. b) The nonorganized phase. The fact that the peak at 6.5 eV is almost nonexistent, the lack of a peak at 291 eV, and the fact that the peak at 284 eV is not well separated are all indications of an amorphous phase. Oxygen was detected in the 532 and 541 eV peaks.

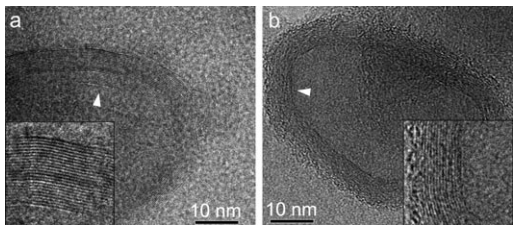

Figure 5. TEM images of a) modern and b) fossilized charcoal samples of the rounded, porous structures (inset shows an enlargement of the region marked by the arrow).

Oxygen was not detected in these ordered structures. We observed that at low magnification the fossilized samples tended to be rounded and have unusual curled structures (Figure 3d) that are rarely seen in the modern samples (Figure 1d).

A detailed examination of the onion-like spherical structures in the HRTEM images in Figure 5 shows that the outer layers of the structure seem to be less ordered than the inner layers in the fossilized charcoal samples. However, in the modern charcoal specimens, the external and internal layers seem to be equally ordered, which suggests that degradation may occur through a layer-by-layer degradation process, from the outside to the core. Unlike the graphite-like microcrystallite sheets in which oxidation occurs at the edges,[27] in the onion-like structures oxidation probably only occurs at defect points along the layers.[28] As the defects in the layers are less abundant than at the edges, the oxidation probably proceeds much faster in the graphite sheets than in the rounded, ordered structures; this would explain the absence of graphite-like sheets and the presence of only a few large rounded, ordered structures in the fossilized samples. On the other hand, the fossilized oak sample (*Quercus*) is uniformly composed of amorphous carbon that contains oxygen. The lack of an organized phase can be explained by considering the *Quercus* modern charcoal composition. The oxidation process is probably faster in this phase compared with the larger organized phases because its structure has a small diameter and is composed of thin (2–4 layers) graphite crystallites, and its EELS spectra indicate some amorphous carbon character (the semiordered structure). We note that the decrease in the amount of ordered (or semiordered) structures in fossilized charcoal is consistent with the bulk properties of fossilized charcoal when compared with modern charcoal.[7]

EELS spectra also revealed the presence of oxygen in the amorphous phase of the fossilized samples and not in the ordered phase. This result reveals that charcoal degradation occurred by means of oxidation in the nonorganized phase. We can only surmise that because most of the ordered phase is missing, it was almost entirely degraded by means of oxidation, which raises the question as to whether the degraded graphite-like microcrystallites are converted into amorphous carbon or not. Although we do not have direct evidence for this, this hypothesis could account for the increase in the relative proportion of the amorphous phase relative to the organized phase in fossilized versus modern charcoals. The amorphous phase has been likened to a humic acid-like material, which is a complex organic material found in soils. It is interesting to note that in some cases, graphite-like microcrystallites were found as part of soil humic acid structures.[7,29,30]

The reduction in the amount of graphite-like microcrystallites and the existence of oxygen in the fossilized samples are consistent with the notion that degradation occurs mainly through oxidation processes. It is possible that the rounded structures in the fossilized samples are more stable than the microcrystallite sheets because they are less susceptible to oxidation.

Conclusion

The different phases of the modern-wood charcoal structure were characterized by means of HRTEM and EELS. We identified two different structural types of charcoal. A two-phase structure composed of organized and nonorganized phases was found in charcoal from two different tree species. This structural type contains large amounts of the nonorganized phase, which accounts for the high resistivity in the bulk material. The second structural type is a homogeneous semiordered structure that is characteristic of nongraphitizing carbon, which contains a small amount of nonorganized phase and exhibits low resistivity in the bulk material. The fossilized samples are dominated by the amorphous phase, which contains oxygen according to analysis by using EELS. These results show that the major degradation mechanism is oxidation, which degrades the graphite-like sheets and alters the amorphous phase. Four out of five samples contained an additional partially organized phase that is mainly present as rounded, hollow structures or as curled structures that are not common in the modern samples, and are probably more stable structures that are less prone to oxidation.

Experimental Section

Modern charcoal sample preparation: A series of modern charcoal samples from different tree species (carob (*Ceratonia siliqua*), bay (*Laurus nobilis*), olive (*Olea europaea*), and oak (*Quercus caliprinos*)) were produced in open fires on a clean rocky substrate. Sections of tree trunks and thick branches were dried for several days in the summer sun prior to burning. The average maximum temperature reached during burning was 920 °C.[31] They were treated with 1 N aqueous HCl to remove the remaining ash, washed twice with deionized water, centrifuged at 3000 rpm, and finally dried in an oven at 60 °C. The samples were homogenized by gentle crushing and grinding in an agate mortar and pestle, and then sieved to < 250 μm. These samples were then characterized.[7]

Fossilized charcoal sample preparation: The samples are from the Iron Age strata of Tel Dor, Israel (3000 BC, sample CHI-5)[32] and the Mousterian and early Upper Paleolithic strata of Kebara Cave, Israel (50000–40000 BC, samples CH-4, CH-16, F-19, and an identified fossilized oak (*Quercus*)).[33] The latter are from the southern part of the cave. These represent two extreme archaeological environments of preservation. Tel Dor sediments almost always contain calcite, which is indicative of an alkaline environment, whereas in Kebara Cave only the sediments in the northern part of the cave contain calcite. The sediments in the center and southern parts contain authigenic phosphate minerals, which indicate that the paleo-pH was once around 4 to 5.[31]

Each sample was analyzed as a single piece of charcoal. The samples were homogenized by gentle crushing and grinding in an agate mortar and pestle, and then sieved to less then 250 μm. The samples were divided into two parts, one part was left untreated and the other was treated with 1 N aqueous HCl for half an hour to dissolve associated minerals such as calcite. The treated samples were cleaned with deionized water and dried; this was repeated and the weight loss was noted.

EELS: The charcoal samples were powdered and dispersed in an ultrasonic bath by means of floating in a Cup Horn to avoid heating (Heat Systems, Farmingdale, NY) for 3 min in ethanol. After an additional 2 min to allow the heavy particles to settle, a drop of the supernatant was placed on a holey carbon-coated TEM grid. Each sample was analyzed twice and in each grid 10 to 15 different locations were examined. The

particles were observed by using an FEI Tecnai-F30 (300 KeV-FEG) microscope equipped with a Gatan imaging filter (GIF). Crystalline areas were first found by using the electron diffraction mode, and then high-resolution images were taken. Finally, the EELS spectra from the ordered and associated disordered phases were recorded. The GIF entrance aperture was 2 mm and the energy resolution was 1.2 eV. EELS measurements were carried out in diffraction coupling mode, on regions of 20–50 nm in thickness and approximately 20 nm in diameter. Owing to the anisotropy of graphite, measurement conditions were set up to a collection semiangle of 3.4 mrad (tested with pure graphite reference sample) to avoid (or minimize) orientation effects of the ELNES.[34] Spectra were analyzed by using Digital Micrograph (Gatan) software.[35] Background interference was removed by means of fitting the data to a power law in the pre-edge region. For thick areas, deconvolution of the edge with the low-loss spectrum was done by using the Fourier-ratio method to eliminate multiple-scattering effects.

Acknowledgements

This study was funded by the Kimmel Center for Archaeological Science at the Weizmann Institute of Science, as well as a generous gift from George Schwartzmann.

[1] S. R. James, *Current Anthropology* **1989**, *30*, 1–11.
[2] I. Thery-Parisot, *J. Archaeol. Sci.* **2002**, *29*, 1415–1421.
[3] S. Thiebault, *Proc. Indian Natl. Sci. Acad. Part A* **1988**, *54*, 501–509.
[4] E. A. Olson, W. S. Broecker, *Trans. N. Y. Acad. Sci.* **1958**, *20*, 593–604.
[5] M. I. Bird, L. K. Ayliffe, K. Fifield, C. S. M. Turney, R. G. Cresswell, T. T. Barrows, B. David, *Radiocarbon* **1999**, *41*, 127–140.
[6] A. C. Scott, *Paleogeography, Paleoclimatology, Paleoecology* **2000**, *164*, 281–329.
[7] I. Cohen-Ofri, L. Weiner, E. Boaretto, G. Mintz, S. Weiner, *J. Archaeol. Sci.* **2006**, *33*, 428–439.
[8] M. I. Bird, C. S. M. Turney, K. Fifield, R. Jones, L. K. Ayliffe, A. Palmer, R. Cresswell, S. Robertson, *Quat. Sci. Rev.* **2002**, *21*, 1061–1075.
[9] A. Oberlin, *Carbon* **1984**, *22*, 521–541.
[10] B. McEnaney, *Carbon* **1988**, *26*, 267–274.
[11] H. C. Foley, *Microporous Mater.* **1995**, *4*, 407–433.
[12] R. E. Franklin, *Proc. R. Soc. London, Ser. A* **1951**, *209*, 196–218.
[13] K. Ishimaru, T. Vystavel, P. Bronsveld, T. Hata, Y. Imamura, J. D. Hosson, *J. Wood Sci.* **2001**, *47*, 414–416.
[14] T. Hata, Y. Imamura, E. Kobayashi, K. Yamane, K. Kikuchi, *J. Wood Sci.* **2000**, *46*, 89–92.
[15] C. E. Byrne, D. C. Nagle, *Carbon* **1997**, *35*, 267–273.
[16] R. Bacon, M. M. Tang, *Carbon* **1964**, *2*, 221-224.
[17] O. Paris, C. Zollfrank, G. A. Zickler, *Carbon* **2005**, *43*, 53–66.
[18] A. S. Livingston, *J. Archaeol. Sci.* **2001**, *28*, 991–1003.
[19] U. Baruch, E. Werker, O. Bar-Yosef, *Actual. Bot.* **1992**, *139*, 531–538.
[20] R. F. Egerton, M. J. Whelan, *J. Electron Spectrosc. Relat. Phenom.* **1974**, *3*, 232–236.
[21] J. J. Ritsko, R. W. Bigelow, *J. Chem. Phys.* **1978**, *69*, 4162–4169.
[22] J. H. Fink, *Adv. Electron. Electron Phys.* **1989**, *75*, 121–232.
[23] J. Yuan, L. M. Brown, *Micron* **2000**, *31*, 515–525.
[24] P. J. F. Harris, A. Burian, S. Duber, *Philos. Mag. Lett.* **2000**, *80*, 381–386.
[25] V. Jeanne-Rose, V. Golabkan, J. L. Mansot, L. Largitte, T. Cesaire, A. Ouensanga, *J. Microsc.* **2003**, *210*, 53–59.
[26] K. Varlot, J. M. Martin, C. Quet, Y. Kihn, *Ultramicroscopy* **1997**, *68*, 123–133.
[27] R. Schlogl, *Surface Composition and Structure of Active Carbon*, Wiley-VCH, Weinheim, **2002**.
[28] A. Tracz, G. Wegner, J. P. Rabe, *Langmuir* **1993**, *9*, 3033–3038.
[29] L. Haumaier, W. Zech, *Org. Geochem.* **1995**, *23*, 191–196.
[30] H. Shindo, T. Higashi, Y. Matsui, *Soil Sci. Plant Nutr.* **1986**, *32*, 579–586.
[31] S. Schiegl, P. Goldberg, O. Bar-Yosef, S. Weiner, *J. Archaeol. Sci.* **1996**, *23*, 763–781.
[32] E. Stern, *Dor—Ruler of the Seas*, 2nd ed., Israel Exploration Society, Jerusalem, **2000**.
[33] O. Bar-Yosef, B. Vandermeersch, B. Arensburg, A. Belfer-Cohen, P. Goldberg, H. Laville, L. Meignen, Y. Rak, D. Speth, E. Tchernov, A. M. Tillier, S. Weiner, *Current Anthropology* **1992**, *33*, 497–550.
[34] R. D. Leapman, P. L. Fejes, J. Silcox, *Phys. Rev. B* **1983**, *28*, 2361–2375.
[35] EELS analysis module: Digital Micrograph, Gatan, Inc., Warrendale, PA (USA); www.gatan.com/analysis/gif_2002.html.

Received: June 28, 2006
Revised: October 24, 2006
Published online: December 13, 2006

